Original Article

Apparent diffusion coefficient; is it an effective index for differentiating between types of lung cancer brain metastases?

Mustafa Devran Aybar, Onder Turna[1]

Department of Radiology, Private Medigold Sultan Hospital, [1]Department of Radiology, Mehmet Akif Ersoy Training and Research Hospital, Istanbul, Turkey

Abstract

Background: The apparent diffusion coefficient (ADC) values of tumors are highly correlated with tumor cellularity and used as a neuroimaging marker with the potential to differentiate between major histological subtypes. Here, we will attempt to determine the sensitivity and specificity of the ADC to distinguish between types of metastatic brain metastases from lung cancer.

Methods: One hundred and fifty-six patients (136 [%87, 18] male, 20 [%12.82] female) admitted to our hospital with the diagnosis of primary lung cancer were included in the study. In addition to conventional magnetic resonance imaging sequences, Diffusion-weighted imaging (DWI) and ADC images were evaluated qualitatively and quantitatively.

Results: We found hyperintensity in most of the metastatic lesions on a qualitatively evaluated DWI sequence. In quantitative assessment according to ADC value comparisons between the different histologic subtype metastatic lung carcinoma groups, small-cell carcinoma (SCLC) had the highest value (1.93×10^{-3}mm^2/s $\pm$ 0.95) and nonsmall-cell-combined (NSCCLC) type was the least (0.55×10^{-3} mm^2/s $\pm$ 0.46). When we tried to distinguish lung cancer-induced brain metastases into two main groups as SCC and NSC by considering the mean ADC ratios we obtained 0.65 $\pm$ 0.14 for SCC and 1.51 $\pm$ 0.30 for NSC. On the other hand, there was no significant statistical difference between the specific histological subtype groups with comparison of ADC values ($P > 0.05$).

Conclusion: Quantitatively quantified DWI-ADC can distinguish metastatic lesions from the normal brain parenchyma. Although we realized whether differentiation of SCLC and non-SCLC in brain metastases can be achieved with DWI, we could not define any correlation between DWI/ADC values and primary histology of the metastatic foci. We believe that more accurate results can be achieved with advanced studies with more patients included and common sequence features.

Keywords: Apparent diffusion coefficient, diffusion-weighted imaging, lung cancer, metastasis, magnetic resonance imaging, metastatic brain tumor

Address for correspondence: Dr. Mustafa Devran Aybar, Department of Radiology, Private Medigold Sultan Hospital, Istanbul, Turkey.
E-mail: mdaybar@gmail.com

Submitted: 21-May-2021 **Revised:** 03-Dec-2021 **Accepted:** 24-Jan-2022 **Published:** 22-Feb-2024

Access this article online	
Quick Response Code:	Website: https://journals.lww.com/wajr
	DOI: 10.4103/wajr.wajr_18_21

How to cite this article: Aybar MD, Turna O. Apparent diffusion coefficient; is it an effective index for differentiating between types of lung cancer brain metastases? West Afr J Radiol 2022;29:84-90.

INTRODUCTION

Metastasis is the most common intracranial tumor in adults.[1] The incidence of central nervous system metastases is approximately 8.3/100,000/year, similar to primary brain neoplasms.[2] The most common types of cancers are lung, breast, colon cancers, malignant melanoma, and paranasal sinus cancers.[1,3,4] In patients with known primary cancer, multiple cerebral lesions indicate metastasis rather than primary brain neoplasm. If the patient does not have a primary cancer history, it is difficult to differentiate metastasis from other glial tumors. Although lung cancers are responsible for 40%–60% of brain metastases, half of the lung cancer cases are lost due to brain metastasis. The majority of lung cancer cases with brain metastasis are small-cell lung cancers.[5,6]

Although diffusion-weighted imaging (DWI) is a contrast-free technique, it was previously used only in the early diagnosis of stroke. DWI has begun to be used for early visualization of cerebral ischemia and has become an indispensable diagnostic tool due to its contributions.[7-10]

Later, with the development of echo-planar imaging with short acquisition times, DWI became available for evaluation of different structures when long acquisition times and draft artifacts were eliminated.[7,11,12] In these studies, apparent diffusion coefficients (ADC) of the requested structures were measured by DWI and it was shown that different values could be used for differential diagnosis. Similarly, there are many studies showing that calculating DWI and ADC values helps conventional magnetic resonance imaging (MRI) in imaging brain tumors.[1,3] Lower ADC values and significantly increased DWI signal intensity (SI) have been demonstrated in high-stage and highly cellular brain neoplasms.[13] In DWI, metastatic tumors of the brain may appear at different signal intensities depending on their histology and cellular content.[2] Statistically, in solid tumor parts, more cell membranes should be included in 1 cm^3 of a small-cell carcinoma (SCLC) than in non-SCLC (NSCLC), because the cytoplasmic diameter is smaller in SCLC.[14] Thus, we predict that the diffusion of water molecules should be less restricted in NSCLC compared to SCLC. We realized whether differentiation of SCLC and NSCLC in brain metastases can be achieved with DWI. The purpose of this study was to determine the diagnostic performance of the ADC values in the discrimination of all types of metastatic brain lesions from lung cancer.

METHODS

Subjects

The patients who have primary lung tumor with brain metastasis admitted to our center between September 2010 and January 2018 were enrolled in the study. This retrospective study was approved by the local ethics committee. Informed written consent was obtained from each patient and the study was performed according to the World Medical Association Declaration of Helsinki. A total of 156 patients with 244 lesions were evaluated. One hundred and thirty-six (%87, 18) of the cases were male and 20 (%12.82) were female. The average age of male cases was 59.8, while the average age of female cases was 55.7. The youngest patient included in the study was 44 years old, while our oldest patient was 84 years old. In the distribution of patients according to histological types, 61 patients (%39.1) had NSCLC, 20 patients (%12.8) had adenocarcinoma (AC), 21 patients (%13.4) had squamous cell carcinoma (SqCC), 40 patients (%25,6) had SCLC (SCLC), seven patients (%4.48) had undetermined malignant type cancer, three patients (%1.92) had large cell carcinoma, two patients (%1.28) had round cell malignant cancer and two patients (%1.28) had small-cell/non-small-cell combined cancer. All of the lung tumors included in our study were diagnosed after being evaluated histopathologically. This evaluation was performed by using bronchial biopsy (96 cases, %61.5), transbronchial, transthoracal needle aspiration (40 cases, %25.6), pleural biopsy (9 cases, %5.76), pleural fluid and bronchial lavage (3 cases, %1.92), lobectomy or pneumonectomy (8 cases, %5.12).

Inclusion criteria were: (1) patients who have primary lung tumor with brain metastases, (2) patients with known histopathological type of lung cancer, (3) patients who have multiple brain metastatic lesions, (4) patients without any history of systemic chemotherapy or local lesion treatments, (5) lesions with sufficient ADC Region of Interest (ROI) images at least 1 cm diameter. **Exclusion criteria were:** (1) patients with general condition disturbances, (2) patients with insufficient respiratory compliances, (3) patients who have had intratumoral hemorrhage, (4) patients who have previously undergone radiotherapy or chemotherapy, (5) patients who have confirmed histological diagnosis of brain tumor.

Two radiology specialists ([MDA] and [OT], over 14 years' experience in MRI diagnostics, blinded to clinical information) independently evaluated the cases and measured the ADC values.

Imaging properties

All MR imaging scans were obtained with a 1.5 T superconducting system (Signa HDxt, GE Medical Systems, Milwaukee, Wisconsin, ABD). Conventional MR imaging and DWI were acquired during the same procedure. Conventional MR imaging study consisted of a axial T1-weighted (TR/TE/NEX/BANDWIDTH=400ms/1ms/0.75/22), sagittal and axial T2-weighted (TR/TE/NEX/BANDWIDTH = 4500ms/100ms/1/40), and axial fluid-attenuated inversion recovery (FLAIR) (TR/TE/NEX/BANDWIDTH = 8000ms/90ms/1/30) sequences, and triplanar contrast-enhanced T1-weighted sequences. The T1-weighted, T2-weighted, and FLAIR sequences were acquired at a section thickness of 5mm with a 1mm intersection gap, a 320×320 matrix, and a 22 cm field of view (FOV). DWI was performed in axial plane using a spin-echo, echo-planar imaging sequence with the following parameters: TR/TE/inversion time, 12000/100/2200; diffusion gradient encoding in 3 orthogonal directions; b = 0 s/mm^2, 500 s/mm^2 and 1000 s/mm^2; FOV, 230–340 mm; matrix size, 128 × 128 pixels; section thickness, 5 mm; section gap, 1 mm; and the number of signals acquired, 1. DWI scans were performed before contrast-enhanced T1-weighted imaging. The ADC values were calculated as follows: ADC = $-(\ln [S/S0])/b$, where S is the SI of the ROI obtained through 3 orthogonally oriented DWIs or diffusion trace images, S_0 is the SI of the ROI acquired through reference T2-weighted images, and b is the gradient b factor with a value of 1000 smm^2. ADC maps were calculated on a pixel-by-pixel basis.

Quantitative evaluation was performed using DWI and ADC images for each case and 30–50 mm^2 of interest (ROI) was selected from metastatic lesions and normal parenchyma. The edema around the masses was excluded from the measurement area while generating the ROI. In the presence of large-sized lesions, 3 separate ROI measurements were averaged.

In addition, the mean ADC value was determined by taking the mean of ADC measurements with successive sections in each lesion**.** In non-homogenous lesions and masses with cystic components, routine and contrast-enhanced sequences were measured from solid areas as possible. Also for determining the ADC ratio, we measured the solid tumor part and the contralateral white mater and divided both values as depicted in our figures. Lesions with a diameter of 1 cm were evaluated with a single ROI. Large lesions were attempted to be measured. In our study of 156 cases, measurements were also made from normal brain parenchyma areas, and mean ADC values were calculated.

Statistical evaluations

While evaluating the study data, as well as descriptive practices methods (Mean, standard deviation), the Pearson-Chi-square test was used to compare qualitative data. Kruskal–Wallis and Unpaired-*t*-test was used to compare quantitative data. The values of ADC mean in the differentiation of different types of tumor lesions were assessed by analyzing the Receiver Operating Characteristic curve and in this regard, the best cut-off value and sensitivity and specificity of each parameter were determined. The software SPSS version 16.0 for windows (SPSS Inc., Chicago, IL, USA) was used to analyze the data. $P < 0.05$ were considered statistically significant.

RESULTS

In the current study, on the distribution of metastases in the brain parenchyma according to their location, the most common metastatic lesion was seen in the frontal lobe (59 cases), followed by the parietal lobe (33 cases) and cerebellum (34 cases) respectively. In 30 cases, metastatic lesions were detected in more than one site. In the distribution of metastatic lesions according to gray-white matter separation, the most common lesion was limited to white matter (70 cases)**.** Metastasis was frequently related to the supratentorial region (74.6%) followed by infratentorial region (18.5%). The size of lesion more than 30 mm was found in 38%. Lesion necrosis was found in 80.0% and most of the patients (95.4%) had edema in their metastatic lesions.

In the distribution of patients according to histological types, 61 patients (%39.1) had NSCLC, 20 patients (%12.8) had adenocarcinoma (AC), 21 patients (%13.4) had SqCC, 40 patients (%25,6) had SCLC, seven patients (%4.48) had undetermined malignant type cancer, three patients (%1.92) had large-cell carcinoma, two patients (%1.28) had round-cell malignant cancer and two patients (%1.28) had small-cell/non-small-cell combined cancer. When the distribution of cases was classified according to gender, NSCLC (56 cases) was most common in males, while adenocarcinoma (12 cases) was more common in females. The mean age was 59.675 ± 9.348 overall and 62 years in NSCLC with the highest number of cases.

Pearson-Chi-square test was used for comparison of primary tumor and DWI signal in visual evaluation performed separately for DWI and ADC. Accordingly, visual assessment and qualitative descriptions of DWI are commonly employed in current practice. In addition, the ADC darkness is less visually sensitive than the DWI brightness on images. DWI hyperintensity was detected

in the majority of tumor lesions and this was statistically significant ($P < 0.005$).

Furthermore, we used ROIs instead of average SI values for DWI of metastatic lesions, since the mean value may downgrade the tumor because of its low-grade area, as metastases are commonly heterogeneous in terms of tissue content. The mean signal intensities obtained from the tumor center, white matter, and homologous normal brain parenchyma. In this evaluation, a significant statistical difference was found between normal brain parenchyma and metastatic tissue DWI ROI measurements ($P < 0.05$). When metastatic lesions were compared among themselves, no statistically significant DWI ROI differences were found ($P > 0.05$). The mean intratumoral ADC value was founded 1.49×10^{-3} mm^2/sn $\pm$ 0.72 while it was 1.20×10^{-3} mm^2/sn $\pm$ 0.30 in normal brain parenchyma. The highest ADC value was founded 1.93×10^{-3} mm^2/sn $\pm$ 0.95 in SCLC [Figure 1].

When we tried to distinguish lung cancer-induced brain metastases into two main groups as SCLC and NSC by considering the mean ADC ratios we obtained 0.65 $\pm$ 0.14 for SCLC and 1.51 $\pm$ 0.30 for NSC. Thus, we observed a significant statistical difference between SCLC and NSC ($P < 0.001$) [Figure 2].

However, regarding the association between the values and the presence of edema, more severe edema in the peritumoral zone was related to significantly higher ADC mean values. Unpaired *t*-test was used when comparing normal brain parenchyma ADC values with metastatic lesions. Accordingly, metastatic lesions and brain parenchyma ADC measurements showed significant differences ($P < 0.05$) [Figures 3 and 4].

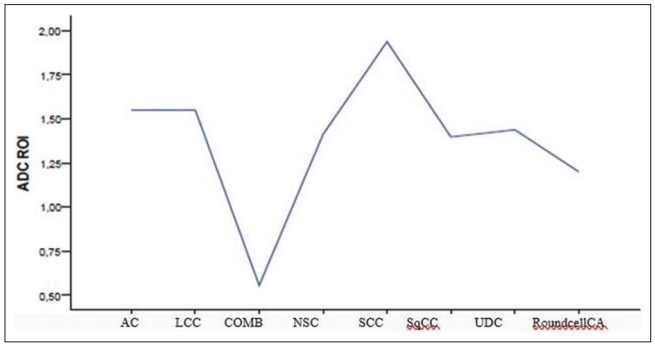

Figure 1: The Kruskal–Wallis test was used to evaluate between groups in metastatic lesions. Accordingly, when the apparent diffusion coefficient values between the groups were compared, no statistically significant difference was found ($P > 0.05$). The highest apparent diffusion coefficient value was founded 1.93×10^{-3} mm^2/sn $\pm$ 0.95 and was seen in small cell carcinoma, the lowest value was seen in nonsmall-cell combined carcinoma (0.55×10^{-3} mm^2/s $\pm$ 0.46)

DISCUSSION

DWI is the technique of diffusion of water molecules (Brownian motions). With DWI, information can be provided on the microscopic structure and regulation of biological tissues and thus pathological changes in different organs and tissues can be identified. The most important clinical use of DWI is in the early detection of cerebral ischemia and is also used in neurological pathologies such as brain tumors, abscesses, white matter diseases.[15] DWI sequences can be obtained by adding diffusion gradients to MRI sequences. Eco Planar Imaging (EPI) is the most important sequence of DWI. EPI is not affected by motion artifacts with its fast viewing time.[15,16] As the b value decreases, the diffusion effect decreases and the T2 effect on the image increases.[17] In our study, we selected the b-value as 1000 sec/mm^2 to dominate the diffusion effect.

The incidence of central nervous system metastases is approximately 8.3/100,000/year, similar to primary brain neoplasms. Malignant brain tumors are composed of high-grade gliomas, metastases, and lymphomas according to high contrast enhancement rates. Contrast agent involvement, tumor-edema, hemorrhage, necrosis, and mass effect are important clues for tumor aggression on conventional MRI.[2]

Although the diagnosis of brain metastatic tumors can be made by clinical history and imaging studies, some metastatic brain lesions cannot be distinguished from high-grade glioma, lymphoma, abscess, tumoral multiple sclerosis and subacute infarct on conventional MRI.[2] If

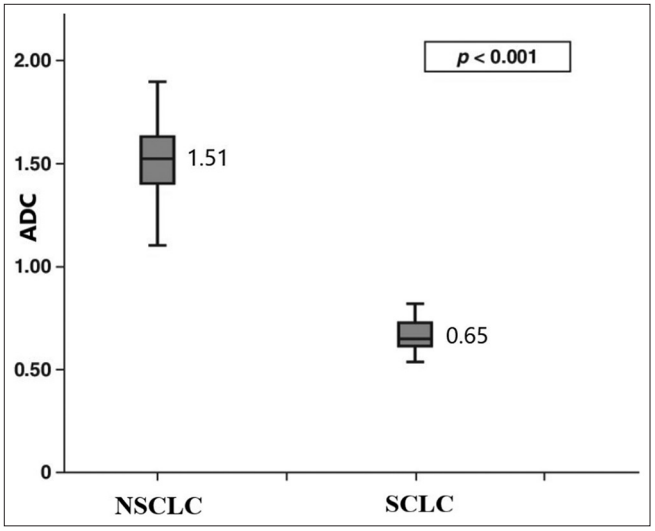

Figure 2: The mean apparent diffusion coefficient ratios (enables differentiation between small cell carcinoma -nonsmall cell carcinoma) were 0.65 $\pm$ 0.14 for small cell carcinoma and 1.51 $\pm$ 0.30 for nonsmall cell carcinoma

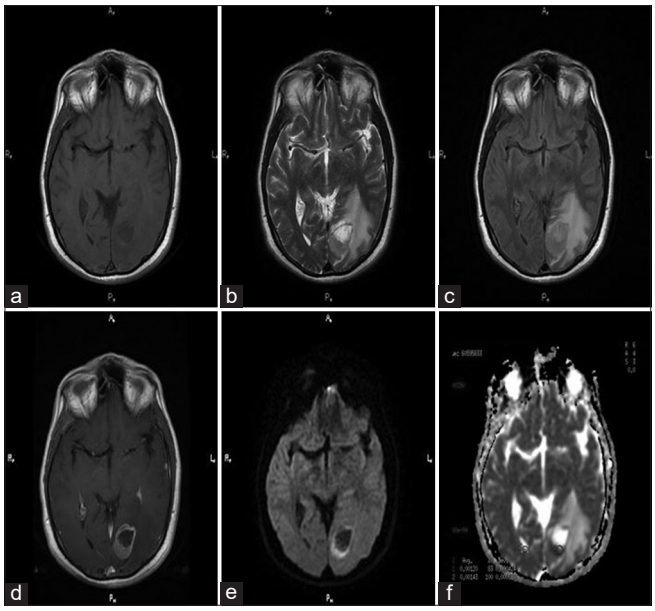

Figure 3: (a) Axial T1WI (b) Axial T2WI (c) fluid-attenuated inversion recovery sequence (d) Axial contrast T1WI (e) Diffusion-weighted imaging (f) Apparent diffusion coefficient images of the 53-year-old male with round cell malignant lung tumor. Large vasogenic edema around the left occipital mediobasal, cortico-subcortical area, measurements were made from the irregularly limited mass lesion with ring and nodular contrast enhancement. apparent diffusion coefficient value calculated 1.26×10^{-3} mm²/sn in this patient

the primary lesion of the patient is known and the lesion is multiple, there is no dilemma in the differentiation of metastasis and malignant tumor in MRI.[13,18] However, if the patient has no history of primary malignancy, it is difficult to distinguish from glioblastoma and anaplastic astrocytoma.[13,19] Brain metastases occur in 8%–10% of cancer patients and are one of the leading causes of cancer-related morbidity and mortality worldwide. The most common types of cancers are lung, breast and colon cancers, malignant melanoma, and paranasal sinus cancers. Lung cancer is responsible for 40%–60% of brain metastases and half of the cases are lost due to progressive brain metastasis. Small-cell lung cancers are the most common metastatic cases. Brain metastases are frequently seen in the skull, leptomeninges, and brain parenchyma. In parenchymal metastases, 80%–85% of the cases are observed in the supratentorial region and high frontal lobe, as in our study.[20]

In the study of Yurdakul *et al.*,[20,21] the parietal lobe was ranked first and the frontal lobe was the second in the distribution of metastatic lesions. Lung tumors developing from brain metastases are mostly located in the upper lungs and peripherally according to the regional distribution.[17] The lesions are 30%–50% solitary in brain metastases due to lung cancer.[5]

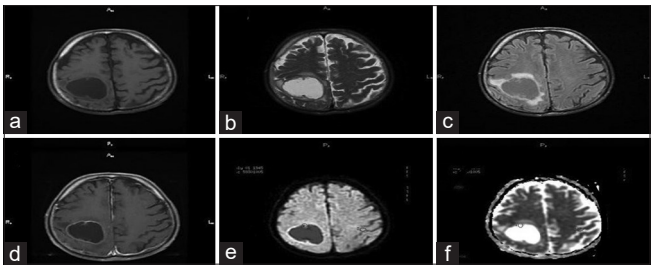

Figure 4: A 66-year-old male with non-small cell lung carcinoma (a) Axial T1WI (b) Axial T2WI (c) Fluid-attenuated inversion recovery sequence (d) Axial contrast T1WI (e) Diffusion-weighted imaging (f) apparent diffusion coefficient images. We had done our measurements in central necrotic peripherally enhancing lesion with surrounding edema, extending from the lateral ventricular level to the right parietal convexity. apparent diffusion coefficient value calculated 1.29×10^{-3} mm²/sn in this patient

Although it has been reported in different studies that SCLC s have low ADC values and appears hyperintense on DWI, the reason for their high signal is still unknown. In their study, Hayashida *et al.*[2] hypothesized that hyperintensities in DWIs had a potent effect of restricted diffusion and T2 brightness. In conclusion, hyperintensity was found in the majority of tumor lesions in our study and this appearance was statistically significant ($P < 0.005$).

Well-differentiated adenocarcinomas in DWI tend to be hypointense compared to gray matter. In addition, they show significantly lower SI than poorly differentiated adenocarcinomas and other histologic types of tumors. In DWI SI is affected by T2, ADC, b value, spin attenuation and TE. Hayashida *et al.*[2] suggested that in their study of b-value and TE stable, all 6 well-differentiated adenocarcinomas showed low SNR and high ADC values at T2WI. Therefore, the hypointensity of well-differentiated adenocarcinomas was attributed to low T2 and high water permeability in tissues, resulting in increased SI on DWI. Furtherly, Hayashida *et al.*[2] evaluated 26 brain metastasis cases, 13 of which were referred to the surgical service after MRI. Metastatic lung, esophagus, breast, synovium, and skin tumors were evaluated in their studies. The intensity of the lesions was defined as 0 isointense, (–) hypointensity, and (+) hyperintensity according to cortical gray matter in DWI. In their studies, they have shown lower SI in well-differentiated adenocarcinomas compared to poorly differentiated and other metastatic lesions. There was no significant difference in mean SI of poorly differentiated adenocarcinomas compared to non-adenocarcinoma lesions. They found stage +2 in three SCLCs and one large cell neuroendocrine carcinoma, and stage-1 SI in one malignant melanoma.[2] In our study, we saw that DWI was variable in metastatic lesions. We reasoned that this variable appearance was due to the altered cellular content and

differentiation of the metastatic lesion and the high SNO ratio of the tissue in T2WI. 44.4% of SCLCs and 64.2% of NSCLCs showed hyperintensity while monitoring. In conclusion, hyperintensity was detected in the majority of tumoral lesions in our study, and this appearance was statistically significant ($P < 0.005$).

ADC values of tumors are highly correlated with tumor cellularity; Hayashida *et al.*[2] in their studies showed a high degree of tumor cellularity in SCLCs and large cell neuroendocrine carcinomas. They also assumed that the cellularity of metastatic brain tumors contributed to ADC values. On the other hand, Çallı *et al.*[13] in their study of 48 cases, and Duygulu *et al.*[1] on 87 cases in which 11 patients with hemorrhagic metastases were excluded, found no statistically significant difference between the ADC values of the group with and without diffusion restriction, supporting our findings and there was no correlation between the metastatic lesion with the primary tumor and the histologic type. In the data of Zakaria *et al.*[22] 2015 study, ADC values were lower for the group of poorly differentiated metastases, such as melanoma and small cell lung cancer, compared to carcinoma metastases (including breast and colorectal). When we made a comparison in terms of ADC values between the groups we considered in our study, the highest ADC value was found in SCLC with 1.93×10^{-3} mm^2/sn $\pm$ 0.95, while the lowest ADC value was found in with/without small-cell combined carcinoma 0.55×10^{-3} mm^2/sn $\pm$ 0.46. When they reviewed data from 129 patients, Müller SJ *et al.*[23] revealed that there would be less diffusion restriction in NSC since SCC has smaller cytoplasmic diameters and will contain more cell membranes in 1 cm^3 area.

We tried to distinguish lung cancer-induced brain metastases into two main groups as SCLC and NSCLC by considering the mean ADC ratios and we obtained 0.65 $\pm$0.14 for SCLC, 1.51$\pm$0.30 for NSCLC. Meyer *et al.*[24] also shared similar data between SCLC and NSCLC in their study in 2015. In summary, we observed a significant statistical difference between SCLC and NSCLC ($P < 0.001$). Thus, we concluded in our study that there is a correlation between the histology of the two main groups of related metastatic lesions according to ADC values. Therewithal values obtained in MRI examination demonstrated that ADC values did not contribute to the diagnosis of tumor type histologies.

In some studies for tumor and brain edema, ADC values of edema and tumor were higher than normal brain parenchyma; central necrosis has been shown to have higher values than tumor lesion, edema, and normal parenchymal structure. Tien *et al.*[25] found that the contrast-enhanced tumor had a significantly lower ADC value than adjacent edema, Brunberg *et al.*[26] found that there was no significant difference between edematous and contrasted tumor. However, both concluded that ADC alone cannot be used to differentiate tumor without contrast enhancement from adjacent edema.[25-27] Since higher ADC values will be obtained in measurements made from the edematous area around the lesion and necrotic components at prior studies,[26-28] we have tried to make measurements outside the edema area and from the solid component showing contrast enhancement.

CONCLUSION

Although the measurement of ADC values, especially on solid parts enables differentiating SCLC and NSC during routine non-invasive MRI examinations, it can be seen that ADC values did not contribute to the diagnosis of detailed tumor type histologies. We believe that further studies considering the common sequence characteristics including more cases, more accurate results will be obtained.

Financial support and sponsorship
Nil.

Conflicts of interest
There are no conflicts of interest.

REFERENCES

1. Duygulu G, Ovali GY, Calli C, Kitis O, Yünten N, Akalin T, *et al.* Intracerebral metastasis showing restricted diffusion: Correlation with histopathologic findings. Eur J Radiol 2010;74:117-20.
2. Hayashida Y, Hirai T, Morishita S, Kitajima M, Murakami R, Korogi Y, *et al.* Diffusion-weighted imaging of metastatic brain tumors: Comparison with histologic type and tumor cellularity. AJNR Am J Neuroradiol 2006;27:1419-25.
3. Liu K, Ma Z, Feng L. Apparent diffusion coefficient as an effective index for the therapeutic efficiency of brain chemoradiotherapy for brain metastases from lung cancer. BMC Med Imaging 2018;18:30.
4. Dirier A, Karadayi B. Comparison of two different radiotherapy schedules in lung cancer patients with brain metastasis. Dicle Med J 2006;33:134-8.
5. Chi A, Komaki R. Treatment of brain metastasis from lung cancer. Cancers (Basel) 2010;2:2100-37.
6. Pellerino A, Internò V, Muscolino E, Mo F, Bruno F, Pronello E. *et al.* Leptomeningeal metastases from non-small cell lung cancer: State of the art and recent advances. J Cancer Metastasis Treat 2020;6:41.
7. Demir OI, Obuz F, Sağol O, Dicle O. Contribution of diffusion-weighted MRI to the differential diagnosis of hepatic masses. Diagn Interv Radiol 2007;13:81-6.
8. van Everdingen KJ, van der Grond J, Kappelle LJ, Ramos LM, Mali WP. Diffusion-weighted magnetic resonance imaging in acute stroke. Stroke 1998;29:1783-90.
9. Back T, Hoehn-Berlage M, Kohno K, Hossmann KA. Diffusion nuclear magnetic resonance imaging in experimental stroke. Correlation with cerebral metabolites. Stroke 1994;25:494-500.
10. Le Bihan D, Turner R, Douek P, Patronas N. Diffusion MR imaging:

Clinical applications. AJR Am J Roentgenol 1992;159:591-9.
11. Yoshikawa T, Kawamitsu H, Mitchell DG, Ohno Y, Ku Y, Seo Y, *et al.* ADC measurement of abdominal organs and lesions using parallel imaging technique. AJR Am J Roentgenol 2006;187:1521-30.
12. Ichikawa T, Haradome H, Hachiya J, Nitatori T, Araki T. Diffusion-weighted MR imaging with a single-shot echoplanar sequence: Detection and characterization of focal hepatic lesions. AJR Am J Roentgenol 1998;170:397-402.
13. Calli C, Kitis O, Yunten N, Yurtseven T, Islekel S, Akalin T. Perfusion and diffusion MR imaging in enhancing malignant cerebral tumors. Eur J Radiol 2006;58:394-403.
14. Vollmer RT. The effect of cell size on the pathologic diagnosis of small and large cell carcinomas of the lung. Cancer 1982;50:1380-3.
15. Dietrich O, Biffar A, Reiser MF, Baur-Melnyk A. Diffusion-weighted imaging of bone marrow. Semin Musculoskelet Radiol 2009;13:134-44.
16. Berghoff AS, Spanberger T, Ilhan-Mutlu A, Magerle M, Hutterer M, Woehrer A, *et al.* Preoperative diffusion-weighted imaging of single brain metastases correlates with patient survival times. PLoS One 2013;8:e55464.
17. Tang G, Liu Y, Li W, Yao J, Li B, Li P. Optimization of b value in diffusion-weighted MRI for the differential diagnosis of benign and malignant vertebral fractures. Skeletal Radiol 2007;36:1035-41.
18. Caravan I, Ciortea CA, Contis A, Lebovici A. Diagnostic value of apparent diffusion coefficient in differentiating between high-grade gliomas and brain metastases. Acta Radiol 2018;59:599-605.
19. Karaarslan E, Arslan A. Diffusion weighted MR imaging in non-infarct lesions of the brain. Eur J Radiol 2008;65:402-16.
20. Yurdakul AS, Calısır HC, Demirag F, Taci N, Ogretensoy M. The distribution of hystological types of lung cancer (Analysis of 2216 cases). Turk Thorac J 2002;3:59-65.
21. Tas SG, Ak H, Ceylan E, Yaycıoglu S, Meteoglu I, Cıldag O. Asymptomatic solitary pons metastasis in small cell lung cancer: A case report. ADU Med Fac J 2009;10:41-3.
22. Zakaria R, Das K, Radon M, Bhojak M, Rudland PR, Sluming V, *et al.* Diffusion-weighted MRI characteristics of the cerebral metastasis to brain boundary predicts patient outcomes. BMC Med Imaging 2014;14:26.
23. Müller SJ, Khadhraoui E, Neef NE, Riedel CH, Ernst M. Differentiation of brain metastases from small and non-small lung cancers using apparent diffusion coefficient (ADC) maps. BMC Med Imaging 2021;21:70.
24. Meyer HJ, Fiedler E, Kornhuber M, Spielmann RP, Surov A. Comparison of diffusion-weighted imaging findings in brain metastases of different origin. Clin Imaging 2015;39:965-9.
25. Tien RD, Felsberg GJ, Friedman H, Brown M, MacFall J. MR imaging of high-grade cerebral gliomas: Value of diffusion-weighted echoplanar pulse sequences. AJR Am J Roentgenol 1994;162:671-7.
26. Brunberg JA, Chenevert TL, McKeever PE, Ross DA, Junck LR, Muraszko KM, *et al. In vivo* MR determination of water diffusion coefficients and diffusion anisotropy: Correlation with structural alteration in gliomas of the cerebral hemispheres. AJNR Am J Neuroradiol 1995;16:361-71.
27. Shaefer PW, Grant PE, Gonzalez RG. Diffusion weighted MR imaging of the brain. Radiology 2000;217:331-45.
28. Han C, Huang S, Guo J, Zhuang X, Han H. Use of a high b-value for diffusion weighted imaging of peritumoral regions to differentiate high-grade gliomas and solitary metastases. J Magn Reson Imaging 2015;42:80-6.